

# Angular profile of Particle Emission from a Higher-dimensional Black Hole: Analytic Results

Panagiota Kanti and Nikolaos Pappas

*Division of Theoretical Physics, Department of Physics,  
University of Ioannina, Ioannina GR-451 10,  
Greece*

## Abstract

During the spin-down phase of the life of a higher-dimensional black hole, the emission of particles on the brane exhibits a strong angular variation with respect to the rotation axis of the black hole. It has been suggested that this angular variation is the observable that could disentangle the dependence of the radiation spectra on the number of extra dimensions and angular momentum of the black hole. Working in the low-energy regime, we have employed analytical formulae for the greybody factors, angular eigenvalues and eigenfunctions of fermions and gauge bosons, and studied the characteristics of the corresponding angular profiles of emission spectra in terms of only a few dominant partial modes. We have confirmed that, in the low-energy channel, the emitted gauge bosons become aligned to the rotation axis of the produced black hole while fermions form an angle with the rotation axis whose exact value depends on the angular-momentum of the black hole. In the case of scalar fields, we demonstrated the existence of a “spherically-symmetric zone” that is followed by the concentration of the emission on the equatorial plane, again in total agreement with the exact numerical results.

# 1 Introduction

Under the assumption that a low-energy scale for gravity exists in the context of a higher-dimensional fundamental theory [1], the possibility of observing in the near future quantum-gravity effects has excited a lot of interest among high-energy physicists, both theorists and experimentalists. The main reason for that is the fact that, if  $M_*$  – the fundamental gravity scale – is as low as a few TeV, then these effects could be observed during trans-Planckian particle collisions at current, ground-based accelerators [2]. One such strong-gravity effect could be the creation of higher-dimensional miniature black holes during the collision of ordinary Standard-Model particles localised on our brane – a (3+1)-dimensional hypersurface embedded in the  $(4 + n)$ -dimensional spacetime, the bulk. Due to their small size, these black holes will have a high temperature and will evaporate very quickly via Hawking radiation [3], i.e. the emission of ordinary particles with a thermal spectrum [4, 5, 6].

The emission of Hawking radiation is anticipated to take place during the two intermediate phases in the life of the black hole, the spin-down and the Schwarzschild phase. It is expected to be the main observable signal not only of the creation of these miniature black holes but of the existence of the extra spacelike dimensions themselves in the absence of which the creation of the former would not be possible. As a result, the study of the emission of Hawking radiation by higher-dimensional black holes has been intense during the last ten years. In the early days, the Schwarzschild phase – the spherically-symmetric phase in the life of the black hole arising presumably after the shedding of its angular momentum – was considered to be the longest and thus the most important. It was also the one with the simplest metric tensor describing the spacetime around it, and therefore the first one to be exhaustively studied both analytically [7, 8] and numerically [9, 10]. The results derived showed a strong dependence of the emission rates of all types of Standard Model particles on the brane on the number of spacelike dimensions existing transversely to the brane <sup>1</sup>.

One was thus led to hope that by detecting the emission of Hawking radiation could not only shed light on aspects arising from the interplay between classical gravity and quantum physics but also give a quantitative answer to a century-old fundamental question, that of the dimensionality of spacetime. Nevertheless, the Schwarzschild phase is preceded by the axially-symmetric spin-down phase. The gravitational background around a simply-rotating black hole – one of the very few cases where the equations of motion of the propagating particles can be decoupled and solved – depends also on the angular-momentum parameter  $a$  of the black hole. According to the results existing in the literature [14, 15, 16, 17, 18, 19, 20, 21, 22, 23, 24, 25, 26], this dependence is carried over in the form of the radiation emission spectra and is, in fact, found to be similar to the effect that the number of additional spacelike dimensions  $n$  has on them. To complicate things more, simulations of black hole events [27, 28] have revealed that the spin-down phase is not a short-lived one, as previously thought, and that the rotation of the black hole remains significant for most of its lifetime.

The fact that the dependence of the radiation spectra on the number of extra dimensions  $n$  for all types of particles is entangled with the dependence on the angular-momentum parameter  $a$  means that measuring both of these parameters is extremely difficult. The only way out was

---

<sup>1</sup>Variants of the spherically-symmetric Schwarzschild phase, where a cosmological constant [11] or the higher-curvature Gauss-Bonnet term [12] were introduced, were also studied with the spectrum exhibiting a dependence also on parameters related to these terms. In addition, the Schwarzschild phase of quantum-corrected black holes has been studied in [13].

to employ another observable that would strongly depend on only one of these two parameters while being insensitive to the other. Upon determination of that particular parameter, the second could then be determined from the radiation spectra. One characteristic feature of the emission spectra coming from the spin-down phase is the non-isotropic emission, in contrast to the one coming from the Schwarzschild phase where the emitted particles are evenly distributed over a  $4\pi$  solid angle. It has therefore been suggested [29, 30] that this non-isotropy can serve as the additional observable necessary to disentangle the  $n$  and  $a$ -dependence of the spectra. Indeed, it was demonstrated [30] that the angular profile of the emitted radiation depends extremely weakly on the number of additional dimensions  $n$  while it may provide valuable information on the angular momentum of the black hole (see, for example, [31]).

More specifically, under the combined effect of the centrifugal force exerted on the emitted particles and the spin-rotation coupling for particles with non-zero spin (an analytical explanation of the latter is given in [32]), the orientation of the emitted radiation depends strongly on the energy channel in which the particles are emitted and on how fast the black hole rotates. If we look specifically at the low-energy channel, then we observe that gauge bosons and fermions have a distinctly different behaviour: the emitted gauge bosons remain aligned to the rotation axis of the black hole independently of the angular-momentum parameter; fermions, on the other hand, form an angle with the rotation axis whose value strongly depends on the value of  $a$ . As a result, the orientation of gauge bosons can serve as a good indicator of the rotation axis of the black hole [30] and the orientation of fermions can then provide a measurement of the value of the angular momentum of the black hole [29, 30].

The aforementioned results presented in [29, 30] were derived by means of a very complicated and time-consuming process that involved the numerical integration of both the radial and angular part of the equation of motion of each emitted particle as well as additional challenges such as the numerical calculation of the angular eigenvalue itself, which does not exist in closed form for a rotating background, and the summation of a very large number of partial modes. The purpose of this work is to provide an alternative way of deriving the angular profile of the emitted radiation without resorting to complicated numerical calculations. This is facilitated by the fact that all valuable information that may be derived from the angular spectra is restricted in the low-energy regime where the radial equations for all types of particles have been analytically solved [18, 19]. In addition, analytical formulae, in the form of power series, for the angular eigenfunction and eigenvalue exist in the literature. By combining all the above in a constructive way, we investigate which contributions are the dominant ones, that predominantly determine the angular profile of the emitted radiation. In this way, we formulate simple constraints involving a finite number of terms and partial modes that successfully reproduce all the features of the anisotropic emission, namely the value of the angle where the emission becomes maximum and the corresponding value of the energy emission rate.

The structure of this paper is as follows. In section 2, we present the theoretical framework with the field equations that need to be solved and the corresponding energy emission rates for a general spin- $s$  field. In section 3, we present the analytical formulae for the greybody factors, angular eigenfunctions and eigenvalues that will be our tools for the analytical investigation of the angular profile of the emitted radiation. In section 4, we consider separately the cases of fermions, gauge bosons and, for completeness, scalar fields too, emitted by a higher-dimensional simply-rotating black hole on the brane: in each case, we determine the dominant modes, formulate simple extremization constraints with respect to the angle of emission  $\theta$ , and derive their angular distribution on the brane. Finally, in section 5, we summarise our results and present our conclusions.

## 2 Theoretical framework

The most generic type of a black hole in a higher-dimensional spacetime is the one that rotates around one or more axes. The gravitational field around such a black hole is described by the Myers-Perry solution [33]. However, it is only for particular configurations of the angular-momentum components that the equation of motion of a particle propagating in the higher-dimensional spacetime can be decoupled into an angular and a radial part. The case of a simply-rotating black hole, where the black hole possesses only one angular-momentum component that lies on a plane parallel to our brane, corresponds to one of these configurations and the one that has been mostly considered in the literature. This choice is also justified by the assumption that the black hole, if created by the collision of two brane-localised particles, will acquire an angular momentum component along the (3+1)-dimensional part of the full manifold.

In this work, we will also focus on the case of a simply-rotating black hole. In addition, we will study effects that take place strictly on our brane, namely the emission of Hawking radiation by the higher-dimensional, rotating black hole in the form of non-zero-spin Standard-Model fields. The line-element of the brane background in which these particles propagate is given by the expression [4]

$$ds^2 = - \left(1 - \frac{\mu}{\Sigma r^{n-1}}\right) dt^2 - \frac{2a\mu \sin^2 \theta}{\Sigma r^{n-1}} dt d\varphi + \left(r^2 + a^2 + \frac{a^2 \mu \sin^2 \theta}{\Sigma r^{n-1}}\right) \sin^2 \theta d\varphi^2 + \frac{\Sigma}{\Delta} dr^2 + \Sigma d\theta^2, \quad (1)$$

where

$$\Delta = r^2 + a^2 - \frac{\mu}{r^{n-1}}, \quad \Sigma = r^2 + a^2 \cos^2 \theta. \quad (2)$$

The mass  $M_{BH}$  of the black hole and its angular momentum  $J$  are related to the  $\mu$  and  $a$  parameters, respectively, through the relations

$$M_{BH} = \frac{(n+2)A_{n+2}}{16\pi G} \mu, \quad J = \frac{2}{n+2} M_{BH} a, \quad (3)$$

where  $A_{n+2} = 2\pi^{(n+3)/2}/\Gamma[(n+3)/2]$  is the area of an  $(n+2)$ -dimensional unit sphere, and  $G$  is the  $(4+n)$ -dimensional Newton's constant. The horizon radius  $r_h$  follows from the equation  $\Delta(r) = 0$ : for  $n \geq 1$ , it may be shown that there is only one real, positive root, which may be implicitly written as  $r_h^{n+1} = \mu/(1+a_*^2)$ , where  $a_*$  is defined as  $a_* \equiv a/r_h$ .

The derivation of the field equations that the brane-localized Standard-Model fields satisfy in the above background follows the analysis performed originally by Teukolsky in 4 dimensions [34]. The method demands the use of the Newman-Penrose formalism and results in a 'master' partial differential equation that scalars, fermions and gauge bosons obey on the brane. If we use a factorized ansatz for the field perturbation  $\Psi_h$  of the form

$$\Psi_h(t, r, \theta, \varphi) = \sum_{\Lambda} {}_h a_{\Lambda} {}_h R_{\Lambda}(r) {}_h S_{\Lambda}(\theta) e^{-i\omega t} e^{im\varphi}, \quad (4)$$

the aforementioned 'master' equation separates, in the background of Eq. (1), into two decoupled ordinary differential equations, a radial

$$\Delta^{-h} \frac{d}{dr} \left( \Delta^{h+1} \frac{d {}_h R_{\Lambda}}{dr} \right) + \left[ \frac{K^2 - ihK\Delta'(r)}{\Delta} + 4ih\omega r + h(\Delta''(r) - 2)\delta_{h,|h|} - h\lambda_{\Lambda} \right] {}_h R_{\Lambda} = 0, \quad (5)$$

and an angular one

$$\frac{d}{dx} \left[ (1-x^2) \frac{d {}_h S_\Lambda(x)}{dx} \right] + \left[ a^2 \omega^2 x^2 - 2ha\omega x - \frac{(m+hx)^2}{1-x^2} + h + {}_h A_\Lambda \right] {}_h S_\Lambda(x) = 0. \quad (6)$$

In the above,  $h$  is the spin-weight,  $h = (-|s|, +|s|)$ , of the given field that distinguishes its radiative components, and  $\Lambda = \{lm\omega\}$  denotes the set of ‘quantum numbers’ of each mode. We have also defined the quantities  $K \equiv (r^2 + a^2)\omega - am$  and  $x \equiv \cos\theta$ . Finally,  ${}_h A_\Lambda$  is the eigenvalue of the spin-weighted spheroidal harmonics  ${}_h S_\Lambda(x)$  - as we will shortly comment, the value of this constant does not exist in closed form. This quantity also determines the separation constant between the radial and angular equations with  ${}_h \lambda_\Lambda \equiv {}_h A_\Lambda - 2ma\omega + a^2\omega^2$ .

The above set of equations has been used in the literature in order to study the emission of Hawking radiation, in the form of an arbitrary spin- $s$  field, from a higher-dimensional, simply-rotating black hole on the brane [14, 15, 17]. The resulting differential energy emission rate per unit time, energy and angle of emission is given by the expression [14, 15]

$$\frac{d^3 E}{d(\cos\theta) dt d\omega} = \frac{1 + \delta_{|s|,1}}{4\pi} \sum_{l,m} \frac{\omega}{\exp(\tilde{\omega}/T_H) \pm 1} \mathbf{T}_\Lambda (-{}_h S_\Lambda^2 + {}_h S_\Lambda^2). \quad (7)$$

The radiation spectrum of the black hole resembles those of a black body with a temperature

$$T_H = \frac{(n+1) + (n-1)a_*^2}{4\pi(1+a_*^2)r_h}. \quad (8)$$

At the same time, however, the spectrum is significantly modified compared to the black-body one: in the exponent, the combination  $\tilde{\omega} = \omega - am/(a^2 + r_h^2)$ , includes the effect of the rotation of the black hole; also, the quantity  $\mathbf{T}_\Lambda$ , the transmission probability (or, greybody factor), determines the number of particles that eventually overcome the gravitational barrier of the black hole and reach asymptotic infinity. If Eq. (7) is integrated over all angles of emission  $\theta$ , we obtain the power rate in terms of unit time and energy

$$\frac{d^2 E}{dt d\omega} = \frac{1 + \delta_{|s|,1}}{2\pi} \sum_{l=|s|}^{\infty} \sum_{m=-l}^{+l} \frac{\omega}{\exp(\tilde{\omega}/T_H) \pm 1} \mathbf{T}_\Lambda. \quad (9)$$

The derivation of the integrated-over-all-angles power spectra, for all species of brane-localised fields – scalars, fermions and gauge bosons, was performed both analytically [18, 19] and numerically [14, 15, 17]. According to these results, the energy emission rate – as well as the particle and angular-momentum emission rates – are significantly enhanced as both the number of additional, spacelike dimensions and the angular-momentum of the black hole increase. The enhancement factor was of order  $\mathcal{O}(100)$  when  $n$  varied between 1 and 6, and of order  $\mathcal{O}(10)$  as  $a_*$  increased from zero towards its maximum value  $a_*^{max} = (n+2)/2$ .

In contrast to the case of the spherically-symmetric Schwarzschild phase, the emission of particles during the rotating phase of the life of the black hole is not isotropic. The axis of rotation introduces a preferred direction in space and the emitted radiation exhibits an angular variation as  $\theta$  ranges from 0 to  $\pi$ . It was found [14, 15, 17] that a centrifugal force is exerted on all species of particles, that becomes stronger as either  $\omega$  or  $a$  increases and forces the particles to be emitted along the equatorial plane ( $\theta = \pi/2$ ). In addition, for particles with non-vanishing spin, an additional force, sourced by the spin-rotation coupling, aligns the

emitted particles parallel or antiparallel to the rotation axis of the black hole – this effect is more dominant the smaller the energy and larger the spin of the particle is. If the form (7) of the power spectrum is used where both helicities appear, the spectrum is symmetric over the two hemispheres,  $\theta \in [0, \pi/2]$  and  $[\pi/2, \pi]$ . If a modified form, in which only one of the helicities appear each time, is used instead, then the angular profile is asymmetric with particles with positive helicity (corresponding to  $_{-|s|}S_{\Lambda}^2$ ) being emitted in the upper hemisphere and particles of negative helicity (corresponding to  $_{+|s|}S_{\Lambda}^2$ ) being emitted in the lower one. This angular variation in the Hawking radiation spectra is considered to be one of the main observable effects on the brane of a higher-dimensional, rotating, decaying black hole.

One would ideally like to deduce the values of both spacetime parameters,  $n$  and  $a$ , from the predicted forms of the Hawking radiation spectra. However, the fact that both parameters affect the integrated-over-all-angles spectra in a similar way impose a great obstacle. The resolution of this problem would demand the existence of an observable that depends strongly on only one of the two parameters while being (almost) insensitive to the other. That observable was shown [29, 30] to be the angular variation of the spectra discussed above. Particularly, in the low-energy channel, the alignment of the gauge bosons along the rotation axis can reveal the orientation of the angular-momentum of the black hole. Then, it was demonstrated that the angle of emission of fermions, in the same energy channel, is very sensitive to the value of the angular-momentum of the black hole: the larger the  $a$  parameter is, the larger the value of  $\theta$ , around which the emission is peaked, becomes. Remarkably, the behaviour of gauge bosons and fermions alike remains unaltered as the dimensionality of spacetime changes.

### 3 Analytical forms of the radial and angular functions

The results on the angular profile of the emitted fields with non-zero spin on the brane, discussed above, were derived by numerically integrating both the radial (5) and the angular (6) equation: the latter in order to find the angular eigenvalue  ${}_hA_{\Lambda}$  and eigenfunction  ${}_hS_{\Lambda}$ , and the former in order to determine the greybody factor  $\mathbf{T}_{\Lambda}$  through the radial function  ${}_hR_{\Lambda}$ . The numerical manipulation of the radial and angular differential equations is necessary for the derivation of the exact solutions for  ${}_hR_{\Lambda}$  and  ${}_hS_{\Lambda}$ , respectively, and subsequently of the complete Hawking radiation spectra. However, when it comes to the spectra of gauge bosons and fermions revealing information about the orientation of axis and value of the angular momentum of the black hole, the range of interest is the low-energy one. Thus, in what follows we will focus on the low-energy channel, and attempt to derive analytically information about the angular profile of non-zero-spin fields emitted on the brane. To this end, we will henceforth ignore the single-component scalar fields and concentrate our study on brane-localised fields with spin 1/2 and 1.

Under the assumption of low-energy of the emitted field and low-angular-momentum of the black hole, the radial equation (5) was analytically solved in [18, 19] for all species of particles. A well-known approximation method was used in which the radial equation was solved first near the horizon, then at asymptotic infinity, and the two were finally matched at an intermediate regime to construct the complete solution for  ${}_hR_{\Lambda}$ . The transmission probability  $\mathbf{T}_{\Lambda}$  for fermions was defined as the ratio of the flux of particles at the black-hole horizon over the one at infinity, with the flux being determined through the conserved particle current. For gauge bosons, where no conserved particle current exists, a radial function redefinition and a simultaneous change of the radial coordinate conveniently change the corresponding gravitational potential to a short-range one - then, the amplitudes of the outgoing and incoming plane waves at infinity

can easily determine the transmission probability. For fermions and gauge bosons,  $\mathbf{T}_\Lambda$  comes out to have the form [19]

$$\mathbf{T}_\Lambda^{(1/2)} = 1 - \frac{4\omega^2}{\frac{1}{2}A_\Lambda + 1 + a^2\omega^2} \left| \frac{Y_{\frac{1}{2}}^{(out)}}{Y_{\frac{1}{2}}^{(in)}} \right|^2 \quad (10)$$

and

$$\mathbf{T}_\Lambda^{(1)} = 1 - \frac{16\omega^4}{(A_\Lambda + 2 + a^2\omega^2)^2} \left| \frac{Y_1^{(out)}}{Y_1^{(in)}} \right|^2, \quad (11)$$

respectively, where

$$\frac{Y_h^{(out)}}{Y_h^{(in)}} = \frac{\Gamma(1+Z) \Gamma\left(\frac{1}{2} + h + \frac{Z}{2}\right)}{(2i\omega)^{2h} \Gamma\left(\frac{1}{2} - h + \frac{Z}{2}\right) \left[ \Gamma(1+Z) e^{i\pi\left(\frac{1}{2}-h+\frac{Z}{2}\right)} + B \Gamma\left(\frac{1}{2} + h + \frac{Z}{2}\right) \right]}. \quad (12)$$

and

$$B \equiv \frac{\Gamma(Z)}{\Gamma\left(\frac{1}{2} - h + \frac{Z}{2}\right)} \frac{\Gamma(c-a-b)\Gamma(a)\Gamma(b)}{\Gamma(c-a)\Gamma(c-b)\Gamma(a+b-c)} \frac{[(1+a_*^2)r_h^{n+1}]^{2\beta+|s|+B_*-2}}{(2i\omega)^Z} \quad (13)$$

In the above, the quantity  $Z$ , defined by

$$Z = \sqrt{(2|s| - 1)^2 + 4(hA_\Lambda + 2|s| + a^2\omega^2)}, \quad (14)$$

appears in the solution of the radial equation in the asymptotic infinity that is expressed in terms of the Kummer functions  $M$  and  $U$ . Similarly, the coefficients  $(a, b, c)$ , given by

$$a = \alpha + \beta + D_* - 1, \quad b = \alpha + \beta, \quad c = 1 - |s| + 2\alpha, \quad (15)$$

are the coefficients of the hypergeometric function  $F$  in terms of which the solution of the radial equation is written near the black-hole horizon. Finally, the following definitions hold [19]

$$D_* \equiv 1 - |s| + \frac{2|s| + n(1+a_*^2)}{A_*} - \frac{4a_*^2}{A_*^2}, \quad \alpha = \frac{|s|}{2} - \left( \frac{iK_*}{A_*} + \frac{h}{2} \right), \quad (16)$$

$$\beta = \frac{1}{2} \left[ (2 - |s| - D_*) - \sqrt{(D_* + |s| - 2)^2 - \frac{4K_*^2 - 4ihK_*A_*}{A_*^2} - \frac{4(4ih\omega_* - h\tilde{\lambda}_\Lambda)(1+a_*^2)}{A_*^2}} \right]. \quad (17)$$

supplemented by the following ones:  $A_* = n + 1 + (n - 1)a_*^2$ ,  $K_* = K/r_h$  and  $h\tilde{\lambda}_\Lambda = h\lambda_\Lambda + 2|s|$ .

For scalar fields, the transmission probability is again defined from the amplitudes of the outgoing and ingoing spherical waves at infinity [18]

$$\mathbf{T}_\Lambda^{(0)} = 1 - \left| \frac{B - i}{B + i} \right|^2 = \frac{2i(B^* - B)}{BB^* + i(B^* - B) + 1}, \quad (18)$$

where  $B$  now is given by the expression

$$B = -\frac{1}{\pi} \frac{Z 2^{2l}}{\left[ \omega r_h (1 + a_*^2)^{\frac{1}{n+1}} \right]^{2l+1}} \frac{\Gamma^2(Z/2) \Gamma(\alpha + \beta + D_* - 1) \Gamma(\alpha + \beta) \Gamma(2 - 2\beta - D_*)}{\Gamma(2\beta + D_* - 2) \Gamma(2 + \alpha - \beta - D_*) \Gamma(1 + \alpha - \beta)}. \quad (19)$$

We note that the angular eigenvalue  ${}_h A_\Lambda$  makes its appearance in the above analytic results both in Eq. (14) and Eq. (17). As already mentioned in the previous section, in the case of a rotating black hole, this quantity does not exist in closed form. For arbitrary large values of the energy of the emitted particle and angular momentum of the black hole, its value can be determined only via numerical means - that was the method applied in [14, 15] where the complete spectra for scalars, fermions and gauge bosons were derived. However, for low  $\omega$  and low  $a$ , the angular eigenvalue of the spin-weighted spheroidal harmonics can be expressed as a power series with respect to  $a\omega$  [35, 36, 37, 38, 39]

$${}_h A_\Lambda = \sum_{k=0}^{\infty} f_k (a\omega)^k. \quad (20)$$

By using the above power-series form for the angular eigenvalue and keeping terms up to fourth order, the analytically derived formulae for the transmission probabilities (10) and (11) for fermions and gauge bosons - as well as the one for scalar fields - were shown in [18, 19] to be in excellent agreement with the exact numerical ones derived in [14, 15]. The power-series expansion of the angular eigenvalue is quite cumbersome and, up to the sixth order, can be found in [35, 36, 37, 38, 39]. It is worth giving here, some particularly simple formulae we have derived, for the needs of our analysis, for the eigenvalues of fermions and gauge bosons up to second order, namely

$${}_{\frac{1}{2}} A_\Lambda = l(l+1) - \frac{3}{4} - \frac{m(a\omega)}{2l(l+1)} + \left\{ \frac{\mathcal{A}_{1/2}^2 + \mathcal{B}_{1/2}^2}{2l(l+1)} - \frac{1}{2} + \frac{m^2}{8} \left[ \frac{1}{(l+1)^3} - \frac{1}{l^3} \right] \right\} (a\omega)^2 + \dots \quad (21)$$

and

$$\begin{aligned} {}_1 A_\Lambda &= l(l+1) - 2 - \frac{2m(a\omega)}{l(l+1)} + \left\{ 2(\mathcal{A}_1^2 + \mathcal{B}_1^2) \left[ 1 - \frac{3}{l(l+1)} \right] \right. \\ &\quad \left. - 2m^2 \left[ \frac{3(l+2)}{(l+1)^3} - \frac{2l+3}{l^3(l+1)^2} \right] + (3-2l-2l^2) \right\} \frac{(a\omega)^2}{(2l+3)(2l-1)} + \dots, \end{aligned} \quad (22)$$

where

$$\mathcal{A}_h = \max(|m|, |s|), \quad \mathcal{B}_h = \frac{mh}{\max(|m|, |s|)}. \quad (23)$$

In the above, we have given the values of the angular eigenvalues for the positive helicities  $h = 1/2$  and  $h = 1$ , respectively. The angular eigenvalues exhibit a well-known symmetry [40, 39] according to which, if  ${}_{|s|} A_\Lambda$  is the eigenvalue for the positive-helicity component of a given field, then the one for the negative helicity  ${}_{-|s|} A_\Lambda$  readily follows from the relation  ${}_{-|s|} A_\Lambda = {}_{|s|} A_\Lambda + 2|s|$ . For completeness, we add here a similar formula for the angular eigenvalue of scalar fields that first appeared in [6]:

$${}_0 A_\Lambda = l(l+1) + \left[ \frac{1-2l-2(l^2-m^2)}{(2l-1)(2l+3)} \right] (a\omega)^2 + \dots \quad (24)$$

Let us now turn to the angular equation (6). Leaver [40] found an analytic solution for the angular eigenfunction  ${}_h S_\Lambda(x)$  that may be expressed as a series of the following form

$${}_h S_\Lambda(x) = e^{a\omega x} (1+x)^{k-} (1-x)^{k+} \sum_{p=0}^{\infty} a_p (1+x)^p, \quad (25)$$



where  $x = \cos \theta$  and  $k_{\pm} \equiv |m \pm h|/2$ . The expansion coefficients  $a_p$  can be found through a three-term recursion relation

$$\alpha_0 a_1 + \beta_0 a_0 = 0, \quad (26)$$

$$\alpha_p a_{p+1} + \beta_p a_p + \gamma_p a_{p-1} = 0, \quad (p = 1, 2, \dots) \quad (27)$$

In the above, the coefficients  $(\alpha_p, \beta_p, \gamma_p)$  are in turn determined by the relations

$$\begin{aligned} \alpha_p &= -2(p+1)(p+2k_-+1), \\ \beta_p &= p(p-1) + 2p(k_-+k_++1-2a\omega) - [a^2\omega^2 + h(h+1) + {}_hA_{\Lambda}] \\ &\quad - [2a\omega(2k_-+h+1) - (k_-+k_+)(k_-+k_++1)], \\ \gamma_p &= 2a\omega(p+k_-+k_++h). \end{aligned} \quad (28)$$

The above analytic form determines the angular eigenfunction up to a constant that can be fixed by imposing the normalization condition  $\int_{-1}^1 |{}_hS_{\Lambda}(x)|^2 dx = 1$ . According to [39], an excellent approximation to the exact solution is obtained by keeping  $\sim 10$  terms in the expansion of (25).

## 4 Analytical description of the angular profile

In this section, we will attempt to study the angular profile of the emitted Hawking radiation on the brane by employing semi-analytic techniques. Our starting point will be Eq. (7) that determines the angular profile of the emitted radiation as a function of  $x = \cos \theta$ . By using the analytical formulae presented in the previous section, we will compute the value of the angle  $\theta$  where the emission of particles becomes maximum. Since the emission of positive and negative helicity components is symmetric under the change  $\theta \rightarrow \pi - \theta$  [30], in what follows we consider only the emission of positive helicity components,  $h > 0$ .

In Eq. (7), the dependence on the angle  $\theta$  is restricted in the angular eigenfunction  ${}_hS_{\Lambda}(x)$ . One may then naively try to extremize this equation to find a constraint that will determine the desired value of  $\theta_{\max}$ , defined as the value of the angle where the differential rate of emission takes its maximum value. We then obtain

$$\frac{d}{dx} \left( \frac{d^3 E}{dx dt d\omega} \right) = \frac{1 + \delta_{|s|,1}}{4\pi} \sum_{l,m} \frac{\omega}{\exp(\tilde{\omega}/T_H) \pm 1} \mathbf{T}_{\Lambda} \left( 2 {}_hS_{\Lambda} \frac{d {}_hS_{\Lambda}}{dx} \right) = 0. \quad (29)$$

By employing the analytical expression (25) for the angular eigenfunction  ${}_hS_{\Lambda}(x)$  and evaluating the derivative, we obtain the following constraint

$$\sum_{l,m} {}_hW_{\Lambda} (1+x)^{2k_-} (1-x)^{2k_+} \sum_{p=0}^{\infty} a_p (1+x)^p \sum_{q=0}^{\infty} a_q (1+x)^q \left( a\omega + \frac{k_-+q}{1+x} - \frac{k_+}{1-x} \right) = 0. \quad (30)$$

In the above, we have defined the ‘‘weight factor’’  ${}_hW_{\Lambda}$  as

$${}_hW_{\Lambda} \equiv \frac{\omega}{\exp[(\omega - m\Omega)/T_H] \pm 1} \mathbf{T}_{\Lambda}. \quad (31)$$

The analytical evaluation of the constraint (30) in full is not possible. As mentioned above, the sum over  $p$  (and  $q$ ), originating from the analytic form of the angular eigenfunction,

may be truncated at a finite value, but care must be taken so that the truncated series remains close to the exact solution and the value of  $\theta_{\max}$  is not affected. The constraint contains two additional sums: one with respect to  $l$ , the total angular-momentum number ranging from  $|s|$  to  $\infty$ , and one over  $m$ , the azimuthal angular-momentum number that takes values in the range  $[-l, +l]$ . None of these sums can be discarded: all of the quantities involved, the coefficients  $k_{\pm}$ ,  $a_p$  (and  $a_q$ ), as well as the weight factor  ${}_hW_{\Lambda}$ , depend on both angular-momentum numbers in a non-trivial manner. It is, therefore, the combined contributions of all, in principle, partial modes that determines the angular profile of the emitted radiation. Finally, these contributions do not enter on an equal footing: each mode carries a weight factor  ${}_hW_{\Lambda}$  – defined in Eq. (31) in terms of the ‘thermal/statistics’ function and the greybody factor  $\mathbf{T}_{\Lambda}$  – that determines the magnitude of its contribution to the angular profile.

In what follows, we will attempt to shed light to the important contributions to Eq. (30) that determine the value and location, in terms of the angle  $\theta$ , of the maximum emission rate for fermions and gauge bosons. As the interesting phenomena take place in the low-energy regime, we will use purely analytic expressions for all quantities involved, namely the angular eigenvalue, the angular eigenfunctions and the greybody factor. Having been established in the literature [30] that the orientation of the emission of fermions and gauge bosons is not affected by the value of the number of extra dimensions introduced in the model, we will keep fixed the value of  $n$  and, henceforth, set  $n = 2$ .

## 4.1 Emission of Fermions

We will start with the most phenomenologically interesting case, the emission of fermions. Our strategy will be the following: by using the most complete analytic forms, we will investigate when a particular contribution to the angular profile becomes so small that is irrelevant and can thus be ignored. We will therefore use the power series expansion (20) for the angular eigenvalue up to fourth order in  $(a\omega)$ , the analytic form of the angular eigenfunction given in (25) by keeping terms<sup>2</sup> up to  $p = 10$ , and, at the beginning, allow the angular-momentum numbers  $(l, m)$  to vary over their full range.

In Figs. 1(ab), we depict the differential emission rate (7) per unit time, unit frequency and angle of emission in terms of  $\cos\theta$ , for the case  $\omega_* = 0.5$  and  $a_* = 0.5$  (left plot) and  $a_* = 1.5$  (right plot). The different curves correspond to the derived spectrum where modes up to a certain value of  $l$  (and all values of  $m$  in the range  $[-l, +l]$ ) have been summed up: the lower (blue) curve includes only the  $l = 1/2$  modes, the next (green) one modes up to  $l = 3/2$ , the subsequent (red) one modes up to  $l = 5/2$  and the last (orange) one modes up to  $l = 7/2$ . We observe that the  $l = 7/2$  curve is not even visible as it is completely covered by the  $l = 5/2$  one – the same happens for all higher modes. As a matter of fact, the difference between the  $l = 5/2$  and  $l = 3/2$  curves is also quite small: for the maximum value of the angular momentum considered,  $a_* = 1.5$ , the difference in the value of the emission rate at its maximum and of  $\theta_{\max}$  is of the order of only 1%; for smaller values of  $a_*$ , the errors reduce even more: for  $a_* = 0.5$ , the difference in the value of the emission rate at its maximum drops at the level of 0.08% while  $\theta_{\max}$  is not affected at all. We may thus conclude, that the sum over  $l$  in (30) can be safely truncated at  $l = 3/2$ . The reason for this significant truncation is the

---

<sup>2</sup>We have confirmed that, by keeping terms up to  $p = 10$  in this expansion, the derived values of the angular eigenfunction agree extremely well with the exact numerical ones – as a consistency check, we have successfully reproduced the plots of the angular eigenfunctions appearing in [39, 15].

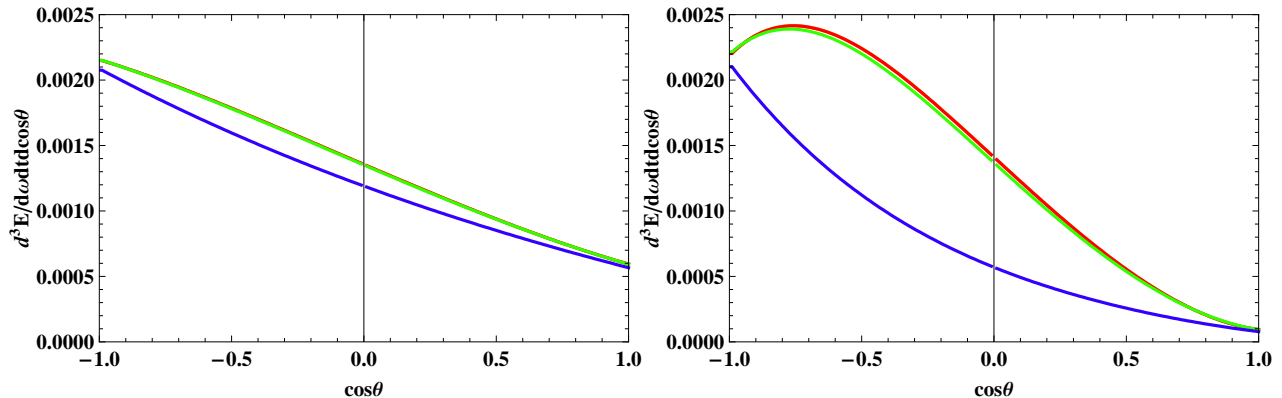


Figure 1: The differential energy emission rate (7) in terms of  $\cos\theta$ , for  $n = 2$ ,  $\omega_* = 0.5$ , and (a)  $a_* = 0.5$  (left plot) and (b)  $a_* = 1.5$  (right plot). The different curves correspond to the emission rate when partial modes up to  $l = 1/2$ ,  $l = 3/2$ ,  $l = 5/2$  and  $l = 7/2$  (from bottom to top) have been summed up.

weight factor  ${}_hW_\Lambda$ : although the thermal/statistics factor gives a boost to modes with large and positive  $m$ , the significant suppression of the greybody factor  $\mathbf{T}_\Lambda$  in the low-energy regime as  $l$  increases ensures that higher modes can be safely ignored.

As a next step in our study, we investigate whether the sum in the series expansion of the eigenfunction can also be truncated. To this end, we have computed the differential energy emission rate (7), for  $\omega_* = 0.5$  and  $a_* = 1$ , by keeping modes up to  $l = 5/2$  for extra safety, and gradually increasing the maximum value of the sum index  $p$ . The behaviour of the corresponding results for the emission rate as a function again of  $\cos\theta$  is plotted in Fig. 2, where the different curves correspond to the maximum value of  $p$  kept in the sum,  $p = 1, 2, 3, 4$  and 10. We observe that the correct value of the emission rate at its maximum is obtained fairly soon, when terms only up to  $p = 2$  are included in the sum; the value of  $\theta_{\max}$ , on the other hand, needs one more term in the expansion ( $p = 3$ ) to acquire its actual value. Our results are not in contradiction with [39] where the value of  $p = 10$  was defined as the one that accurately reproduces the exact form of the eigenfunction. Indeed, higher terms included in the sum up to  $p = 10$  do change the behaviour of the eigenfunction, however, these changes are restricted in the area away from the angle of maximum emission, as Fig. 2 clearly shows. The value of the angular momentum of the black hole strongly affects the value of  $p_{\max}$ : for  $a_* = 1.5$ , the correct value of  $\theta$  is obtained when terms up to  $p = 4$  are included; in contrast, for  $a_* = 0.5$ , no terms higher than  $p = 1$  are needed in the sum.

Let us comment at this point on the expression of the angular eigenvalue that was used in our calculations. As noted above, we initially employed the power series form of Eq. (20) with terms up to the fourth order in  $(a\omega)$ . However, we have found that the expression (21), with terms up to second order only, is more than adequate to lead to accurate results. Although including higher-order terms cause, at times, a significant change in the value of the angular eigenvalue itself, that change hardly affects any aspects of the angular profile of the emitted radiation. For example, for the mode  $l = 1/2$  and  $m = -1/2$ , the difference in the value of the eigenvalue, when terms up to second and third order, respectively, are kept, is of the order of 10%, the effect in the value of the coefficient  $\beta_p$  appearing in Eq. (28) is only 0.2% which leaves the angular profile virtually unchanged.

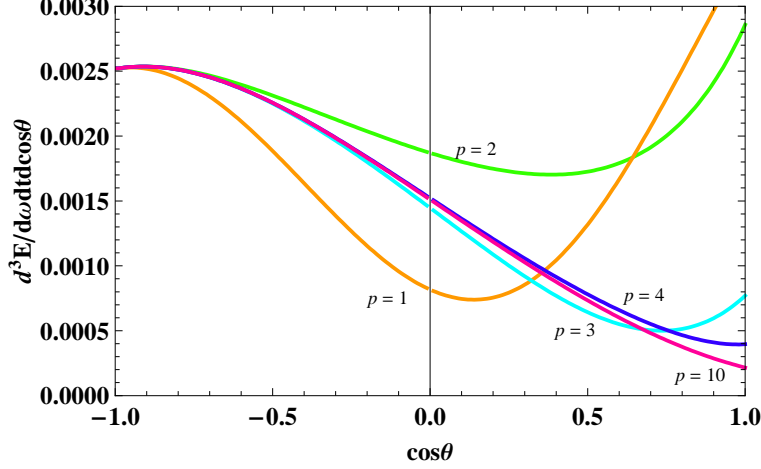


Figure 2: Energy emission rate per unit time, unit frequency and angle of emission in terms of  $\cos\theta$ , for  $n = 2$ ,  $\omega_* = 0.5$  and  $a_* = 1$ , and terms in the series expansion of the angular eigenfunction summed up to  $p = 1$ ,  $p = 2$ ,  $p = 3$ ,  $p = 4$  and  $p = 10$ .

One may simplify further the analysis by considering more carefully the partial modes that dominate the energy emission spectrum. According to the results above, the sum over  $l$  can be safely truncated at the value  $l = 3/2$ , and thus we need to sum over the following six modes:  $(l, m) = [(\frac{1}{2}, \frac{1}{2}), (\frac{1}{2}, -\frac{1}{2}), (\frac{3}{2}, \frac{3}{2}), (\frac{3}{2}, \frac{1}{2}), (\frac{3}{2}, -\frac{1}{2}), (\frac{3}{2}, -\frac{3}{2})]$ . However, not all of the above modes have the same contribution to the angular variation of the energy spectrum. In Fig. 3(a), we display the angular eigenfunctions of the four most dominant modes out of the aforementioned six, for  $n = 2$ ,  $\omega_* = 0.5$  and angular momentum  $a_* = 0.5$  (left plot). It is clear that, for small values of  $a_*$ , the two  $l = 1/2$  modes dominate over the  $l = 3/2$  ones. This dominance is further enhanced when the corresponding weight factors are taken into account, with the ones for the  $l = 3/2$  modes being at least one order of magnitude smaller than the ones for the  $l = 1/2$  modes. But even the contribution of the two dominant modes,  $(\frac{1}{2}, \pm\frac{1}{2})$ , is not of the same magnitude: when the weight factors and the difference in magnitude of the angular eigenfunctions are taken into account, the  $(\frac{1}{2}, \frac{1}{2})$  mode is found to have at least five times bigger contribution than the  $(\frac{1}{2}, -\frac{1}{2})$  one. As a result, the angular pattern of the emitted radiation at the low-energy channel, for small values of the angular momentum parameter, is predominantly defined by the  $(\frac{1}{2}, \frac{1}{2})$  mode. Then, the constraint (30) takes the simplified form <sup>3</sup>

$$\sum_{q=0}^3 a_q (1+x)^q \left( a\omega + \frac{q}{1+x} - \frac{1}{2(1-x)} \right) = 0, \quad (32)$$

and more particularly

$$\left( a\omega - \frac{1}{2(1-x)} \right) \left[ a_0^{(1/2)} + a_1^{(1/2)}(1+x) + a_2^{(1/2)}(1+x)^2 + a_3^{(1/2)}(1+x)^3 \right] \\ + a_1^{(1/2)} + 2a_2^{(1/2)}(1+x) + 3a_3^{(1/2)}(1+x)^2 = 0. \quad (33)$$

In the above, we have used that  $k_- = 0$  and  $k_+ = 1/2$  for the mode  $(\frac{1}{2}, \frac{1}{2})$ , and the superscript  $\{1/2\}$  denotes that the set of coefficients  $a_p^{(1/2)}$  for this particular mode should be used here. In

<sup>3</sup>In what follows, we will adopt the value  $p = 3$  as the maximum value of the sum index needed to accurately reproduce the behavior of the fermionic eigenfunction around the angle of maximum emission.

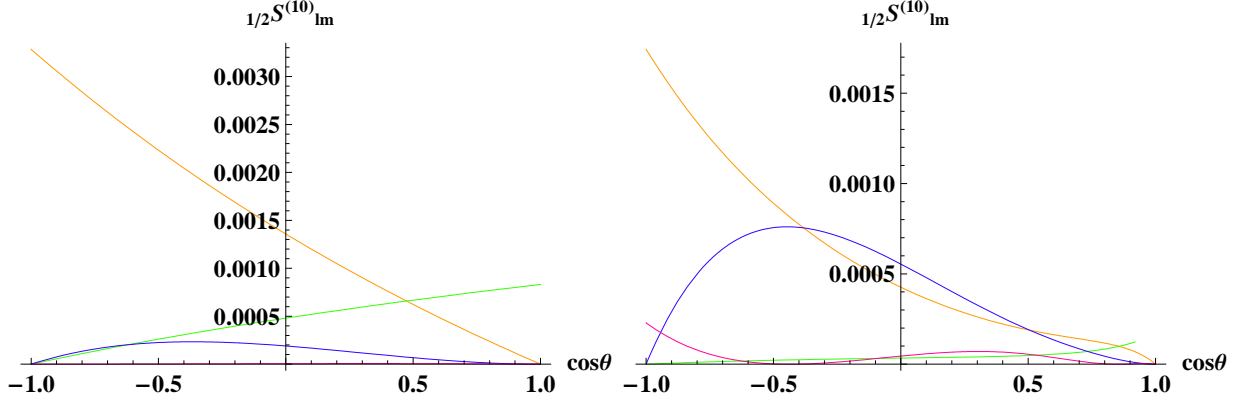


Figure 3: The fermionic angular eigenfunction  ${}_{1/2}S_{lm}^{(10)}$  as a function of  $\cos\theta$ , for  $n = 2$ ,  $\omega_* = 0.5$  and: a)  $a_* = 0.5$  (left plot) and  $(l, m) = [(\frac{1}{2}, \frac{1}{2}), (\frac{1}{2}, -\frac{1}{2}), (\frac{3}{2}, \frac{3}{2}), (\frac{3}{2}, \frac{1}{2})]$  (from top to bottom), b)  $a_* = 1.5$  (right plot) and  $(l, m) = [(\frac{1}{2}, \frac{1}{2}), (\frac{3}{2}, \frac{3}{2}), (\frac{3}{2}, \frac{1}{2}), (\frac{1}{2}, -\frac{1}{2})]$  (from top to bottom).

Appendix A.1, we list the results for the angular eigenvalue, as this follows from Eq. (21), the values of the  $(\alpha_p, \beta_p, \gamma_p)$  coefficients, according to the definitions (28), and finally the relations between the first four sum coefficients  $a_p$ , given by the three-term recursion relations (26)-(27). A simple numerical analysis, then, shows that Eq. (33) does not have any roots in the range  $x \in (-1, +1)$  for  $a\omega < 0.52$ , with the global maximum located at  $x = -1$  and the global minimum at  $x = 1$ . Therefore, if we fix the energy channel at e.g.  $\omega_* = 0.5$ , the angular eigenfunction of the  $(\frac{1}{2}, \frac{1}{2})$ -mode does not show any extrema up to  $a_* \simeq 1$ ; as a result, the energy emission rate takes its maximum value at  $\theta = \pi$  in accordance with the exact numerical results derived in [29, 30].

Nevertheless, as  $a_*$  increases, the  $(\frac{3}{2}, \frac{3}{2})$ -mode becomes important – this may be clearly seen in Fig. 3(b). Let us examine the behaviour of this mode on its own. Its extremization constraint is given now by

$$\left( a\omega + \frac{1}{2(1+x)} - \frac{1}{(1-x)} \right) \left[ a_0^{(3/2)} + a_1^{(3/2)}(1+x) + a_2^{(3/2)}(1+x)^2 + a_3^{(3/2)}(1+x)^3 \right] + a_1^{(3/2)} + 2a_2^{(3/2)}(1+x) + 3a_3^{(3/2)}(1+x)^2 = 0, \quad (34)$$

where we have used that, for this mode,  $k_- = 1/2$  and  $k_+ = 1$ . By making use of the relations between the first four  $a_p^{(3/2)}$  coefficients, as these are found again in Appendix A.1, and performing a simple numerical analysis, we arrive at the following results: for  $a\omega = 0$ , all  $a_i$  with  $i \geq 1$  vanish, and the constraint (34) reveals the existence of a sole extremal point at  $x = -1/3$ ; this extremum is a local maximum – as  $a_*$  increases, the local maximum becomes gradually more important and slowly moves to the left, thus competing with the maximum of the  $(\frac{1}{2}, \frac{1}{2})$ -mode at  $x = -1$  to create a global maximum for the energy emission rate in the range  $(-1, -1/3)$  with the exact location depending on the value of  $a_*$ .

Thus, summarizing the above results, for an arbitrary value of  $a_*$ , the angular variation of the emitted fermions is mainly determined by the contribution of the  $(\frac{1}{2}, \frac{1}{2})$  and  $(\frac{3}{2}, \frac{3}{2})$  modes,

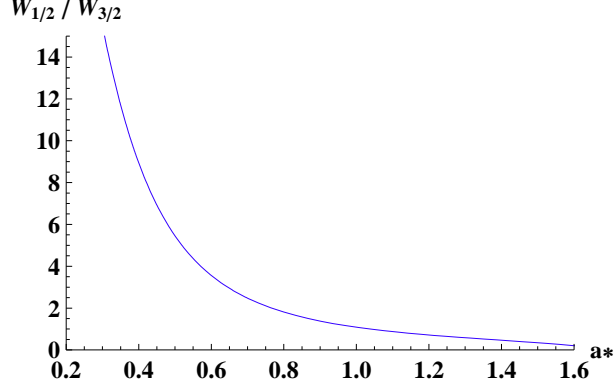


Figure 4: The relative weight factor  $W_{rel} = W_{1/2}/W_{3/2}$  in terms of the angular-momentum parameter  $a_*$ , for the particular case of  $\omega_* = 0.6$ .

and thus the constraint (30) may take the final form

$$\begin{aligned}
W_{rel} \sum_{p=0}^3 a_p^{(1/2)} (1+x)^p \sum_{q=0}^3 a_q^{(1/2)} (1+x)^q \left( a\omega + \frac{q}{1+x} - \frac{1}{2(1-x)} \right) \\
+ (1-x^2) \sum_{p=0}^3 a_p^{(3/2)} (1+x)^p \sum_{q=0}^3 a_q^{(3/2)} (1+x)^q \left( a\omega + \frac{1/2+q}{1+x} - \frac{1}{1-x} \right) = 0. \quad (35)
\end{aligned}$$

We have also defined the relative “weight factor”  $W_{rel} = W_{1/2}/W_{3/2}$  whose value depends strongly on the angular parameter  $a_*$  – this dependence is shown in Fig. 4. For small values of  $a_*$ ,  $W_{rel}$  takes large values and the extremization constraint is dominated by the  $(\frac{1}{2}, \frac{1}{2})$ -mode causing the emitted fermions to be aligned with the rotation axis. As  $a_*$  increases,  $W_{rel}$  decreases reaching the value one for approximately  $a_* = 1$  – now, both modes contribute equally and  $\theta_{max}$  is pushed away from the  $\theta = \pi$  value. For even larger values of  $a_*$ , the  $(\frac{3}{2}, \frac{3}{2})$ -mode starts dominating with the angle of maximum emission moving further away.

In support of our argument, that the  $(\frac{1}{2}, \frac{1}{2})$  and  $(\frac{3}{2}, \frac{3}{2})$  modes predominantly determine the angular variation of the fermionic spectrum, in Table 1 we display the values of the energy emission rate at the angle of maximum emission as well as the value of the corresponding angle  $\theta_{max}$ , for various values of the energy parameter  $\omega_*$  and angular-momentum parameter  $a_*$ . In each case, we display two values: the first one follows by taking into account the contribution of the two aforementioned modes and keeping terms only up to  $p = 3$  in the sum of the angular eigenfunction (or, up to  $p = 4$  for  $a_* \geq 1$ ); the second follows by keeping all terms up to  $p = 10$  and all partial modes up to  $l = 7/2$ . The values of the energy parameter  $\omega_*$  have been chosen to lie in the low-energy regime and, at the same time, to display a non-trivial angular variation of the spectrum – it is worth mentioning that for all values smaller than  $\omega_* = 0.5$ , the angle of maximum emission is constantly located at  $\theta = \pi$ . On the other hand, the angular-momentum parameter  $a_*$  scans a fairly broad range from  $a_* = 0.5$  to  $a_* = 1.5$ .

For the energy channel  $\omega_* = 0.5$ , the agreement between the two sets of results is extremely good: the error in the value of the energy emission rate at its maximum reaches the magnitude of 3.5% at most, while the agreement in the value of  $\theta_{max}$  is perfect. In agreement with the exact numerical results [30] where this energy channel was studied, for small values of  $a_*$ , the emitted radiation remains very close to the rotation axis and only for values close to  $a_* = 1.0$

	$\omega_* = 0.5$		$\omega_* = 0.6$		$\omega_* = 0.7$		$\omega_* = 0.8$	
	approx.	full	approx.	full	approx.	full	approx.	full
$a_* = 0.50$	2.078	2.150	1.956	2.053	1.545	1.657	1.028	1.132
	-0.99	-0.99	-0.99	-0.99	-0.99	-0.89	-0.87	-0.74
$a_* = 0.75$	2.316	2.406	2.054	2.168	1.693	1.827	1.232	1.402
	-0.99	-0.99	-0.82	-0.81	-0.66	-0.64	-0.57	-0.52
$a_* = 1.00$	2.444	2.535	2.170	2.282	1.809	1.970	1.303	1.552
	-0.91	-0.91	-0.68	-0.67	-0.56	-0.54	-0.51	-0.46
$a_* = 1.25$	2.488	2.567	2.090	2.205	1.590	1.784	1.019	1.338
	-0.81	-0.81	-0.61	-0.60	-0.52	-0.50	-0.46	-0.43
$a_* = 1.50$	2.347	2.415	1.715	1.831	1.038	1.248	-	0.098
	-0.76	-0.76	-0.57	-0.56	-0.41	-0.42	-	-0.40

Table 1: The approximated and full values of the energy emission rate (7) at the angle of maximum emission, in units of  $10^{-3}/r_h$ , and the corresponding values of  $\cos(\theta_{\max})$  for fermions.

the emission starts showing a maximum at a gradually smaller angle. For  $\omega_* = 0.6$ , the errors in the value of the emission rate and  $\theta_{\max}$  are at the level of 5% and 3% respectively, with the emission being peaked at an angle away from the horizon axis for  $a_* \geq 0.75$ . For  $\omega_* = 0.7$ , the error in the value of  $\theta_{\max}$  is still quite small <sup>4</sup> ranging between 3% and 4%, whereas the error in the value of the emission rate at its maximum is now taking large values (7%-17%). Finally, for completeness, we show the energy channel of  $\omega_* = 0.8$ : although we have probably exceeded the range of validity of our approximation, the error in the value of  $\theta_{\max}$  remains less than 10%.

The above comparison demonstrates that, for low values of the parameters  $\omega_*$  and  $a_*$  where our semi-analytic approximation is valid, the use of the two modes, the  $(\frac{1}{2}, \frac{1}{2})$  and  $(\frac{3}{2}, \frac{3}{2})$  ones, and the constraint (35) can provide realistic results for the angular variation of the fermionic spectrum. This can consequently help to determine the value of the angular momentum of the black hole according to the proposal of [29, 30]. The results displayed in Table 1 confirm the behaviour found numerically for the energy channel  $\omega_* = 0.5$  [30], extend the set of values that could be used for comparison with experiment to additional low-energy values of  $\omega_*$  and, finally, provide a very satisfactory semi-analytic approximation in terms of only two partial modes.

## 4.2 Emission of Gauge Bosons

Let us now address the emission of gauge bosons on the brane by the simply-rotating black hole. We will again focus on the low-energy regime as this is the energy channel at which the emission of gauge bosons is polarised along the rotation axis of the black hole. We will attempt to determine the main factors that contribute to this behaviour and, if possible, provide analytical arguments that justify it.

<sup>4</sup>The error in the value of  $\theta_{\max}$  is indeed quite small for all values of  $a_* \geq 0.75$ . For  $a_* = 0.5$ , we observe a significant deviation of  $\theta_{\max}$  from its actual value for the energy channels  $\omega_* = 0.7$  and  $\omega_* = 0.8$ . This is due to the fact that, for these specific values of the energy parameter and angular momentum, the mode  $(\frac{1}{2}, -\frac{1}{2})$  that we have ignored in our approximation is of the same order of magnitude as the  $(\frac{3}{2}, \frac{3}{2})$  that we have taken into account.

	$a_* = 0.5$		$a_* = 1.0$		$a_* = 1.5$	
$l_{\max}$	Rate	$\cos(\theta_{\max})$	Rate	$\cos(\theta_{\max})$	Rate	$\cos(\theta_{\max})$
$l = 1$	0.017866	-0.99	0.028779	-0.99	0.066357	-0.99
$l = 2$	0.017883	-0.99	0.028817	-0.99	0.066440	-0.99
$l = 3$	0.017883	-0.99	0.028817	-0.99	0.066440	-0.99
$p_{\max}$	Rate	$\cos(\theta_{\max})$	Rate	$\cos(\theta_{\max})$	Rate	$\cos(\theta_{\max})$
$p = 0$	0.017948	-0.99	0.029051	-0.99	0.067319	-0.99
$p = 1$	0.017866	-0.99	0.028778	-0.99	0.066353	-0.99
$p = 2$	0.017866	-0.99	0.028779	-0.99	0.066357	-0.99
$p = 3$	0.017866	-0.99	0.028779	-0.99	0.066357	-0.99

Table 2: The differential energy emission rates at the maximum angle of emission and the corresponding angle for gauge bosons, for  $\omega_* = 0.3$  and  $n = 2$ , in terms of the angular-momentum number  $l$  and sum index  $p$ , and for three indicative values of  $a_*$ .

Following a similar strategy as in the case of fermions, we first investigate whether the infinite sum over the partial modes, characterised by  $(l, m)$ , in Eq. (30) can be truncated. By gradually increasing the value of  $l$  (and summing over all corresponding values of  $m$ ), we looked for that value beyond which any increase in  $l$  makes no difference to the value of the energy emission rate at its maximum and of the corresponding angle. It turns out that, at the low-energy regime, this value is reached very quickly – this behaviour is clearly displayed by the entries of Table 2. In the upper part of the Table, we present the energy emission rate (7) at its maximum and the corresponding angle as we increase  $l$  from 1 to 3 and vary  $a_*$  from 0.5 to 1.5 in a random low-energy channel ( $\omega_* = 0.3$ ). We observe that the value of the angle of maximum emission for positive-helicity ( $h = 1$ ) gauge bosons is indeed  $\theta = \pi$ , i.e. anti-parallel to the angular-momentum vector of the black hole, and that this value is not affected at all by adding any partial modes beyond the ones with  $l = 1$ . The energy emission rate also varies very little: its value at the angle of maximum emission is already reached for  $l = 2$  and the difference from its value when only the  $l = 1$  modes are taken into account is of the order of 0.1% independently of the value of the angular-momentum of the black hole. We may thus conclude that the angular profile of the emission of gauge bosons at the low-energy regime is determined almost exclusively by the lower  $l = 1$  modes: the sum over  $l$ , therefore, in Eq. (30) can be replaced by the contribution of only its first term.

We performed a similar analysis regarding the value of  $p$  in the sum in the expression for the angular eigenfunction, and we have found similar results displayed in the lower part of Table 2. The value of the angle of maximum emission is again not affected as terms beyond the first one ( $p = 0$ ) are added. The actual value of the energy emission rate at the maximum angle is also very loosely dependent on  $p$ : as  $p$  goes from 1 to 2, the difference is of the order of  $10^{-3}\%$ , while the difference between the cases with  $p = 0$  and  $p = 1$  is again very small, of the order of 0.5%. While, according to the above, the sum over  $p$  can be clearly truncated even at  $p = 0$ , to increase the validity of the subsequent analysis, we will also keep terms with  $p = 1$ , and thus write the analytic expression (25) of the angular eigenfunction as

$${}_1S_\Lambda(x) = e^{a\omega x} (1+x)^{k-} (1-x)^{k+} [a_0 + a_1(1+x)]. \quad (36)$$

A final point that needs to be addressed is the contribution of the different  $m$ -modes. For  $l = 1$ , we have three modes with  $m = +1, 0, -1$  that have, nevertheless, a different weight factor



and thus a different contribution to the constraint (30). A numerical evaluation of the weight factor (31), with  $\mathbf{T}_\Lambda$  given in Eq. (11), for these three modes, in conjunction with the value of the angular eigenfunction in each case, reveals that the contribution of the  $m = 1$  mode to the constraint (30) is almost two orders of magnitude larger than the one of the  $m = 0$  mode, and that in turn is larger by two orders of magnitude than the contribution of the  $m = -1$  mode. Therefore, it is the  $l = m = 1$  mode that effectively determines the angular profile of the emitted radiation.

Then, the constraint (30) can take a particularly simple form. For  $l = m = 1$  and  $h = 1$ , we obtain  $k_- = 0$  and  $k_+ = 1$ , which then leads to the condition

$$a_0 \left( a\omega - \frac{1}{1-x} \right) + a_1 (1+x) \left( a\omega + \frac{1}{1+x} - \frac{1}{1-x} \right) = 0. \quad (37)$$

The above can be written as a quadratic polynomial in  $x$ , with solutions

$$x_{\text{ex}} = - \left( \frac{a_0}{2a_1} + \frac{1}{a\omega} \right) \pm \sqrt{1 + \frac{1}{(a\omega)^2} + \frac{a_0}{a_1} + \frac{a_0^2}{4a_1^2}}. \quad (38)$$

If the above values correspond to extremal points in the regime  $x \in (-1, 1)$ , then they should satisfy the inequality  $|x_{\text{ex}}| < 1$ . This in turn imposes constraints on the coefficients  $a_0$  and  $a_1$ . As in the case of fermions, these coefficients, for a given set of numbers  $(h, l, m)$ , are given solely in terms of the parameter  $a\omega$ . In Appendix A.2, we present the main steps for the derivation of the relations between the sum coefficients  $a_p$  in the case of gauge bosons. There, it is found that, for the mode  $h = l = m = 1$ ,

$$\frac{a_1^{(1)}}{a_0^{(1)}} = -\frac{a\omega}{2} \left( 3 + \frac{9a\omega}{20} \right). \quad (39)$$

We substitute the above ratio into Eq. (38), and demand that  $-1 < x_{\text{ex}} < 1$ . While the left-hand-side inequality is automatically satisfied for all values of  $a\omega$ , the right-hand-side translates to  $9(a\omega)^2 + 60a\omega - 20 > 0$  that leads to the constraint  $a\omega > 0.32$ .

Therefore, for  $a\omega < 0.32$  no extremal points for the differential energy emission rate exist in the range  $x \in (-1, 1)$ . This quantity is thus monotonic and has global extremal points at the end points  $x = -1$  and  $x = +1$ . Substituting  $k_- = 0$  and  $k_+ = 1$  in Eq. (36), it is easy to see that, for  $x = +1$ , the angular eigenfunction vanishes, while, for  $x = -1$ , it takes its maximum value  $2a_0e^{-a\omega}$ . As a result, the positive-helicity component of the gauge field is perfectly aligned in an anti-parallel direction to the angular-momentum vector of the black hole ( $\theta = \pi$ ), in agreement with the exact numerical results [30]. If  $a\omega$  exceeds the value 0.32, a local maximum develops at an internal point of the range  $(-1, 1)$ , however, this remains subdominant to the global maximum at  $x = -1$  up to the value  $a\omega \simeq 0.85$ . Therefore, if we fix the energy channel to  $\omega_* = 0.5$ , the maximum of the emitted radiation in the form of gauge fields remains aligned in an antiparallel direction to the angular-momentum of the black hole for all values of  $a_*$  up to 1.7, in agreement again with the exact numerical results [30].

### 4.3 Emission of Scalars

We finally address the case of the emission of scalar fields on the brane by a simply-rotating black hole. Although no useful information regarding the angular momentum of the black hole

$l_{\max}$	Rate	$\cos(\theta_{\max})$	$p_{\max}$	Rate	$\cos(\theta_{\max})$
$l = 0$	0.00052329	$\pm 1$	$p = 1$	0.00438439	$\pm 1$
$l = 1$	0.00137162	0	$p = 2$	0.00165378	$\pm 0.67$
$l = 2$	0.00139658	0	$p = 3$	0.00135215	$\pm 0.05$
$l = 3$	0.00139688	0	$p = 4$	0.00137489	0
$l = 4$	0.00139688	0	$p = 5$	0.00137122	0
$l = 5$	0.00139688	0	$p = 6$	0.00137167	0

Table 3: The differential energy emission rates at the maximum angle of emission and the corresponding angle, for  $\omega_* = 0.3$ ,  $n = 2$  and  $a_* = 1.5$ , in terms of the angular-momentum number  $l$  and sum index  $p$  for scalar fields.

can be derived in this case, for completeness, we briefly discuss the main characteristics of the angular pattern of the scalar emission and the main contributing factors.

In order to investigate whether it is possible again to truncate the sums over  $l$  and  $p$ , that appear in the constraint (30), we construct Table 3. The left-hand-side of the table displays the energy emission rate at the angle of maximum emission and the corresponding angle in terms of the angular-momentum number  $l$ . The energy channel  $\omega_* = 0.3$  has been chosen as an indicative case, the number of extra dimensions has been again fixed to  $n = 2$ , and the angular-momentum parameter is taken to be  $a_* = 1.5$  – this is the highest value of  $a_*$  considered in this analysis, and the one for which the convergence of the sums over  $l$  and  $p$  is the most difficult to achieve. We observe that all modes beyond  $l = 2$  add a contribution of order 0.01%, and thus can be safely ignored. But the difference between the values of the emission rate when all modes up to  $l = 1$  and  $l = 2$  have been, respectively, summed up is also very small, of the order of 1%. The value of  $\theta_{\max}$  has also been stabilised to  $\pi/2$  when  $l_{\max} = 1$ . Therefore, in the context of our semi-analytic approach, the sum over  $l$  can be indeed truncated at  $l = 1$  with no significant error.

On the right-hand-side of Table 3, we keep all partial modes up to  $l = 2$  for extra accuracy, and examine the convergence of the sum over  $p$ . The change in the value of the energy emission rate at the angle of maximum emission between the cases with  $p = 4$  and  $p = 5$  is of the order of 0.3%, while all higher contributions are an order of magnitude smaller. The value of  $\theta_{\max}$  has also taken the exact value of  $\pi/2$ , therefore this sum can be safely truncated at  $p = 4$ .

An exhaustive analysis of the values of the weight factors of the contributing partial modes  $(l, m) = \{(0, 0), (1, -1), (1, 0), (1, 1)\}$  for a variety of energy channels,  $\omega_* \in (0.2 - 0.8)$  and angular-momentum of the black hole,  $a_* \in (0.5 - 1.5)$ , reveals that the two most dominant modes are the  $(0, 0)$  and  $(1, 1)$  with the contributions of the other two being always two orders of magnitude smaller. Therefore, combining all the above results, the extremization constraint (30) for the case of scalar fields, takes the simplified form:

$$\begin{aligned}
W_{rel} \sum_{p=0}^4 a_p^{(00)} (1+x)^p \sum_{q=0}^4 a_q^{(00)} (1+x)^q \left( a\omega + \frac{q}{1+x} \right) \\
+ \sqrt{1-x^2} \sum_{p=0}^4 a_p^{(11)} (1+x)^p \sum_{q=0}^4 a_q^{(11)} (1+x)^q \left( a\omega + \frac{1/2+q}{1+x} - \frac{1}{2(1-x)} \right) = 0. \quad (40)
\end{aligned}$$

In the above, we have used that for the  $(0, 0)$ -mode,  $k_- = k_+ = 0$ , while for the  $(1, 1)$ -mode,

$k_- = k_+ = 1/2$ . Also, in this case, the relative weight factor is defined as  $W_{rel} \equiv W_{00}/W_{11}$ . The expressions of the sum coefficients  $a_p^{(00)}$  and  $a_p^{(11)}$  for the two modes can be found at the Appendix A.3.

Let us consider individually the two dominant modes. Starting from the  $l = m = 0$  mode, we write its extremization constraint as

$$\sum_{p=0}^3 [a\omega a_p + (p+1) a_{p+1}] (1+x)^p + a\omega a_4 (1+x)^4 = 0. \quad (41)$$

This is a polynomial of fourth degree that in principle has four roots and, therefore, four potential extremal points. However, if we use the expressions of the  $a_p$  coefficients for the  $l = m = 0$  mode listed in Appendix A.3, we find that two of these roots are complex conjugates and one lies outside the range  $[-1, 1]$ . Thus, the angular wavefunction of the  $l = m = 0$  mode has only one extremal point with respect to  $x = \cos \theta$ . This extremum is a minimum located at  $x = 0$  ( $\theta = \pi/2$ ) for small values of  $a\omega$  that moves to positive values of  $x$  as  $a\omega$  increases. However, the latter effect is actually an artifact of the truncation of the sum in the expression of the angular eigenfunction at a finite value of  $p$ . Even in our approximation where terms up to  $p = 4$  are kept, we may see that the constant term of the polynomial (41) is given by a particular combination of the  $a_p$  coefficients that due to multiple cancellations quickly tends to zero, namely

$$\sum_{p=0}^3 [a\omega a_p + (p+1) a_{p+1}] + a\omega a_4 \simeq -\frac{(a\omega)^4}{72} + \mathcal{O}(a\omega)^5. \quad (42)$$

Had we kept all terms in the series expansions of the angular eigenvalue and eigenfunction, every subsequent term in the sum of (42) would cancel part of the remain of all previous ones all the way to infinity, thus ensuring that the  $x = 0$  is always an extremum of the  $l = m = 0$  mode. A simple numerical analysis then shows that this local extremum is the only one in the range  $(-1, 1)$  and corresponds to a minimum. Due to the fact that  $k_+ = k_- = 0$ , the  $l = m = 0$  mode reaches the same maximum value at the boundary points  $x = \pm 1$ .

Moving to the next dominant mode  $l = m = 1$ , its extremization constraint reads

$$\sum_{p=0}^4 a_p (1+x)^p [a\omega (1-x^2) - x(p+1) + p] = 0. \quad (43)$$

This is a polynomial of sixth degree whose six roots are potential extremal points. Substituting the  $a_p$  coefficients for this mode from Appendix A.3 and performing a simple numerical analysis, one may see that the four roots are two pairs of complex conjugate numbers and one lies outside the range  $[-1, 1]$  leaving again only one root that may indeed correspond to a local extremal point of the angular eigenfunction of the  $l = m = 1$  scalar mode with respect to  $x = \cos \theta$ . As in the case of the  $l = m = 0$  mode, the extremum is located at  $x = 0$  and moves towards positive values of  $x$  as the parameter  $a\omega$  increases. We have again confirmed that the constant term of the above polynomial tends again to zero very quickly, i.e.

$$\sum_{p=0}^4 (a\omega + p) a_p \simeq -\frac{(a\omega)^4}{375} + \mathcal{O}(a\omega)^5, \quad (44)$$

signalling the fact that the  $x = 0$  is always an extremum of the angular eigenfunction of the  $l = m = 1$  mode. The difference from the case of the  $l = m = 0$  mode lies in the fact that now

this extremum is a global maximum instead of a minimum with the angular eigenfunction of the  $l = m = 1$  mode vanishing at the boundary points  $x = \pm 1$  since  $k_+ = k_- = 1/2$ . Let us briefly add here that a similar analysis of the remaining two scalar modes,  $l = 1, m = 0$  and  $l = -m = 1$ , shows that these follow the behaviour of the  $l = m = 0$  and  $l = m = 1$  modes, respectively.

The exact numerical analysis of the emission of scalar fields on the brane by a simply-rotating higher-dimensional black hole [14] has revealed that the corresponding spectrum shows no angular variation for low values of the energy parameter  $\omega_*$  and of the angular-momentum number  $a_*$ . Clearly, for  $a_* = 0$ , the constraint (41) is trivially satisfied and the  $l = m = 0$  mode shows no extremal points – note that, for the mode  $l = m = 1$ , the constraint (43) still leads to a maximum at  $x = 0$  even at  $a_* = 0$ . For low values of  $\omega_*$ , a careful analysis reveals that it is the  $l = m = 0$  mode that dominates over the others, therefore, for low  $a_*$ , the spectrum remains spherically-symmetric. As  $a_*$  starts increasing, the  $l = m = 0$  also develops an extremum at  $x = 0$  – it turns out that there is always a low-energy regime where the minima of the  $l = m = 0$  and  $l = 1, m = 0$  modes exactly cancel the maxima of the  $l = m = 1$  and  $l = -m = 1$  modes leading again to a spherically symmetric spectrum, however, this energy regime becomes gradually more narrow. If we allow the energy parameter  $\omega_*$  to increase, too, then fairly quickly the  $l = m = 1$  mode starts dominating causing the spectrum to exhibit maximum emission at  $x = 0$ , i.e. on the equatorial plane ( $\theta = \pi/2$ ), in agreement with the exact numerical results [14].

## 5 Discussion and conclusions

One of the most exciting prospects of the theories predicting the existence of additional spacelike dimensions in nature and a low fundamental scale for gravity is the potential creation of higher-dimensional black holes from the collision of ordinary brane-localised particles. If the scale is low enough, the creation could in principle take place at ground-based particle accelerators and possibly be observed in the near future. The main observable signal is considered to be the emission of Hawking radiation on the brane in the form of ordinary Standard Model particles.

During the study of the spherically-symmetric Schwarzschild phase, it was found that the radiation spectra of higher-dimensional black holes – even if we focus on the part of the emission that takes place on the brane where ourselves, the observers, are located – show a strong dependence on the number of additional spacelike dimensions that exist transversely to our brane. Therefore, the expectation was formed that the detection of the Hawking radiation spectra could lead to the determination of the number of extra spacelike dimensions in nature. However, if the angular-momentum of the black hole is taken into account – which generically is non-zero and seems to dominate almost all of the life of the black hole – this dependence on  $n$  is entangled with the dependence on the angular-momentum parameter  $a$ .

During the spin-down phase of the life of the produced black hole, the emission exhibits, among other features, a strong angular variation in the radiation spectra with respect to the rotation axis of the black hole. It has been suggested [29, 30] that this angular variation is the observable that could disentangle the dependence of the radiation spectra on  $n$  and  $a$  as it depends strongly on the latter while being (almost) insensitive to the former. It was found that, in the low-energy channel, the emitted gauge bosons become aligned to the rotation axis of the produced black hole while fermions form an angle with the rotation axis whose exact

value depends on the angular-momentum of the black hole.

Attacking the problem of the angular variation of the Hawking radiation spectra in an exact way, and for all values of the parameters of the theory, is extremely challenging. It demands the numerical determination of both the radial and angular eigenfunction of the emitted fields as well as the numerical calculation of the angular eigenvalue that connects the corresponding equations. In addition, the angular pattern of the emitted spectra is formed from the contribution of an, in principle, infinite number of partial modes, numbered by the pair of angular-momentum numbers  $(l, m)$ , each entering in the expression of the emission rate with its own weight (thermal and greybody) factor. Therefore, the use of the formal extremization constraint, that we have derived and which should determine the angles of maximum emission of all species of particles, seems rather unrealistic.

Nevertheless, as the exact numerical analyses [29, 30] have shown, all the valuable information that we should deduce from the angular spectra are restricted in the low-energy regime. In this regime, one may use approximate techniques to solve the radial equation and thus determine the weight-factor of each contributing partial mode [18, 19]. In addition, analytic formulae for the angular eigenvalue and eigenfunction exist [35, 36, 37, 38, 39, 40] that allow us to study the problem of the angular variation of the spectra without resorting to complex numerical techniques. Combining the above tools in a constructive but critical manner, we were able to study the angular variation of the Hawking radiation spectra of fermions, gauge bosons and scalar fields in a semi-analytic way.

Starting from the case of fermionic fields, the use of the analytic form of the greybody factor allowed us to compute the weight factor of each contributing partial mode. This, combined with a power series form for both the angular eigenvalue and eigenfunction, led to the isolation of the partial modes that predominantly determine the angular pattern of the corresponding radiation spectra in the low-energy regime. Also, by demanding that the errors associated to the elimination of all higher-order terms were small, we were able to truncate the infinite sums in both the expressions of the angular eigenvalue and eigenfunction. At the end, we demonstrated that the contribution of only two partial modes, the  $(\frac{1}{2}, \frac{1}{2})$  and  $(\frac{3}{2}, \frac{3}{2})$ , was more than adequate to provide approximate results for the value of the angle of maximum emission and of the corresponding emission rate that were within a range of 5% accuracy of the full results. Our study was completed by the derivation of the values of the above quantities, both in an exact and approximate way, for a variety of values of the energy parameter  $\omega_*$  of the emitted fermionic field and angular-momentum parameter  $a_*$  of the black hole, that could in principle be used for the determination of the angular momentum upon the observation of such a radiation spectrum.

Whereas the angular variation of the radiation spectra of the emitted fermions is very sensitive to the value of the angular-momentum of the black hole – the larger the  $a$  parameter is, the larger the value of  $\theta_{\max}$  – the orientation of the gauge bosons emitted in the low-energy regime was found, by the exact numerical analyses, to be constantly aligned to the rotation axis of the black hole. Thus although it seems that no further information can be deduced from the study of the gauge bosons, we nevertheless performed the same analysis in an attempt to justify analytically the predicted behaviour. We demonstrated, by using a similar strategy as in the case of fermions, that a single mode, the  $l = m = 1$ , mainly determines the angular profile of the emitted gauge bosons. As its angular eigenfunction exhibits no extremal points up to  $a\omega = 0.32$ , and even then these extrema remain subdominant to the global maximum at  $\theta = 0, \pi$  (for helicities  $h = \mp 1$ , respectively) up to  $a\omega = 0.85$ , it is thus confirmed that

the emission of gauge bosons in the low-energy regime will remain aligned to the rotation axis of the black hole for a wide range of the angular-momentum parameter. For example, gauge bosons emitted in the energy channel  $\omega_* = 0.5$  will remain mostly parallel or antiparallel to the rotation axis up to the value of  $a_* = 1.7$ , however, they will start deviating significantly from this behaviour for values of the angular momentum parameter of the black hole larger than this.

For completeness, we have finally studied the case of the emission of scalar fields on the brane by a simply-rotating black hole. In this case, the exact numerical analyses have shown that the emission remains spherically-symmetric for low values of  $\omega$  and  $a$  and then, as either of the two parameters increases, the emission starts concentrating on the equatorial plane. One could thus assume that by looking at the emission of scalar fields, the equatorial plane, and thus the rotation axis of the black hole, could again be determined. Our analysis has shown that the angular profile of the radiation spectra of scalars in the low-energy regime is mainly determined by two modes, the  $l = m = 0$  and  $l = m = 1$ , the first having a minimum at  $\theta = \pi/2$  and the second a maximum at the same point. For small values of  $\omega_*$  and  $a_*$ , we have confirmed that the combination of these two modes creates indeed a “spherically-symmetric zone” in the emission where the two extrema exactly cancel each other. As either  $\omega_*$  and  $a_*$  increases further, it is the  $l = m = 1$  mode that starts dominating pushing the bulk of the emitted scalars towards the equatorial plane. Nevertheless, this transition becomes gradually and is finally realised for values of the parameters of the theory where our approximate techniques are not valid any more.

Closing, let us note that our analysis in this work was based on the study of aspects, such as the existence of extremal points and relative magnitudes, of the spin-weighted spheroidal harmonics. These functions arise in a variety of problems, both in four dimensions as well as in the context of brane models, whenever the study of spin- $s$  fields in a 4-dimensional spacetime with one angular-momentum component is performed. We thus envisage that the properties of the angular eigenfunctions revealed in this analysis as well as the analytic expressions of the angular eigenvalues and  $a_p$  coefficients for fermions, gauge bosons and scalar fields presented in the Appendix will be of use in a variety of problems. Nevertheless, let us stress that the aspects of the particular problem studied here, i.e. the angular profile of the emission of Standard Model particles on the brane by a higher-dimensional black hole, could not be performed only by means of 4-dimensional tools: the particles emitted propagate on a brane embedded in a higher-dimensional spacetime, and this is reflected in the expressions of the greybody factors that determine to a great extent the weight factors of the individual partial modes. It is therefore the combination of both traditional 4-dimensional and brane techniques that has allowed us to analytically reproduce the angular distribution of energy emission, and hopefully provide the means for the determination of the angular momentum and axis of rotation of the produced black hole.

## Acknowledgements

The authors would like to thank Marc Casals for his valuable help with the normalization factors of the spin-weighted spheroidal harmonics. This research has been co-financed by the European Union (European Social Fund - ESF) and Greek national funds through the Operational Program "Education and Lifelong Learning" of the National Strategic Reference Framework (NSRF) - Research Funding Program: THALIS. Investing in the society of knowledge through

the European Social Fund.

## A Expansion Coefficients for the Spin-Weighted Spheroidal Harmonics

The three-term recursion relations (26)-(27) can be used to determine the coefficients  $a_p$  that appear in the expansion of the spin-weighted spheroidal harmonics  ${}_h S_\Lambda$ . For instance, for the first five expansion coefficients, we obtain

$$a_1 = -\frac{\beta_0}{\alpha_0} a_0, \quad a_2 = -\frac{\beta_1}{\alpha_1} a_1 - \frac{\gamma_1}{\alpha_1} a_0 = \left( \frac{\beta_1 \beta_0}{\alpha_1 \alpha_0} - \frac{\gamma_1}{\alpha_1} \right) a_0, \quad (45)$$

$$a_3 = -\frac{\beta_2}{\alpha_2} a_2 - \frac{\gamma_2}{\alpha_2} a_1 = \left( -\frac{\beta_2 \beta_1 \beta_0}{\alpha_2 \alpha_1 \alpha_0} + \frac{\beta_2 \gamma_1}{\alpha_2 \alpha_1} + \frac{\gamma_2 \beta_0}{\alpha_2 \alpha_0} \right) a_0, \quad (46)$$

$$a_4 = -\frac{\beta_3}{\alpha_3} a_3 - \frac{\gamma_3}{\alpha_3} a_2 = \left( \frac{\beta_3 \beta_2 \beta_1 \beta_0}{\alpha_3 \alpha_2 \alpha_1 \alpha_0} - \frac{\beta_3 \beta_2 \gamma_1}{\alpha_3 \alpha_2 \alpha_1} - \frac{\beta_3 \gamma_2 \beta_0}{\alpha_3 \alpha_2 \alpha_0} - \frac{\gamma_3 \beta_1 \beta_0}{\alpha_3 \alpha_1 \alpha_0} + \frac{\gamma_3 \gamma_1}{\alpha_3 \alpha_1} \right) a_0. \quad (47)$$

The  $(\alpha_p, \beta_p, \gamma_p)$  coefficients are given by Eqs. (28) and must be evaluated for each specific partial mode.

### A.1 Fermions

For the needs of our analysis, we determine the above coefficients for the fermionic modes  $(\frac{1}{2}, \frac{1}{2})$  and  $(\frac{3}{2}, \frac{3}{2})$ . First, for the  $(\frac{1}{2}, \frac{1}{2})$ -mode, Eq. (21) leads to the following result for the corresponding eigenvalue ( $h = 1/2$ )

$${}_{\frac{1}{2}} A_{\frac{1}{2}\frac{1}{2}} = -\frac{a\omega}{3} - \frac{11}{27} (a\omega)^2, \quad (48)$$

where we have used that, for this mode,  $k_- = 0$  and  $k_+ = 1/2$ . Then, the  $(\alpha_p, \beta_p, \gamma_p)$  coefficients take the form

$$\alpha_p^{(1/2)} = -2(p+1)^2, \quad \beta_p^{(1/2)} = p(p+2) - 4a\omega(p + \frac{2}{3}) - \frac{16}{27} (a\omega)^2, \quad \gamma_p^{(1/2)} = 2a\omega(p+1). \quad (49)$$

Then, the recursion relations (26)-(27) lead to the following relations between the first four sum coefficients

$$\frac{a_1^{(1/2)}}{a_0^{(1/2)}} = -\frac{4}{3} a\omega \left( 1 + \frac{2a\omega}{9} \right), \quad \frac{a_2^{(1/2)}}{a_0^{(1/2)}} = (a\omega)^2 \left( 1 + \frac{28a\omega}{81} \right) + \dots, \quad (50)$$

$$\frac{a_3^{(1/2)}}{a_0^{(1/2)}} = -\frac{392}{729} (a\omega)^3 \left( 1 + \frac{187}{441} a\omega \right) + \dots \quad (51)$$

The superscript (1/2) denotes that the above expressions hold for the case of the  $(\frac{1}{2}, \frac{1}{2})$  partial mode. We have also given only the relations between the first four expansion coefficients since, as shown in section 4.1, in the case of fermions, it suffices to consider only terms up to  $p = 3$  in the sum of Eq. (25).

For the mode  $(\frac{3}{2}, \frac{3}{2})$ , using the fact that now  $k_- = 1/2$  and  $k_+ = 1$ , we arrive at the following result for the angular eigenvalue

$${}_{\frac{1}{2}}A_{\frac{3}{2}\frac{3}{2}} = 3 - \frac{a\omega}{5} - \frac{29}{125}(a\omega)^2. \quad (52)$$

In turn, the  $(\alpha_p, \beta_p, \gamma_p)$  coefficients take the form

$$\alpha_p^{(3/2)} = -2(p+1)(p+2), \quad \beta_p^{(3/2)} = p(p+4) - 4a\omega(p + \frac{6}{5}) - \frac{96}{125}(a\omega)^2, \quad \gamma_p^{(3/2)} = 2a\omega(p+2). \quad (53)$$

Finally, the above result into the following relations between the first four sum coefficients

$$\frac{a_1^{(3/2)}}{a_0^{(3/2)}} = -\frac{6}{5}a\omega \left(1 + \frac{4a\omega}{25}\right), \quad \frac{a_2^{(3/2)}}{a_0^{(3/2)}} = \frac{4}{5}(a\omega)^2 \left(1 + \frac{34a\omega}{125}\right) + \dots, \quad (54)$$

$$\frac{a_3^{(3/2)}}{a_0^{(3/2)}} = -\frac{716}{1875}(a\omega)^3 \left(1 + \frac{1588}{4475}a\omega\right) + \dots. \quad (55)$$

## A.2 Gauge Bosons

We now turn to the case of gauge bosons, and more particularly to the dominant mode with  $h = l = m = 1$ . Employing Eq. (22) and (28), we find the following results for the angular eigenvalue

$${}_1A_{11} = -a\omega - \frac{11}{20}(a\omega)^2, \quad (56)$$

and the  $(\alpha_p, \beta_p, \gamma_p)$  coefficients

$$\alpha_p = -2(p+1)^2, \quad \beta_p = p(p+3) - a\omega(4p+3) - \frac{9(a\omega)^2}{20}, \quad \gamma_p = 2a\omega(p+2). \quad (57)$$

We may then compute the relations between the different sum coefficients  $a_p$  - although for our analysis we need only the relation between  $a_1$  and  $a_0$ , for completeness, we display again the relations between the first four coefficients

$$\frac{a_1^{(1)}}{a_0^{(1)}} = -\frac{a\omega}{2} \left(3 + \frac{9a\omega}{20}\right), \quad \frac{a_2^{(1)}}{a_0^{(1)}} = (a\omega)^2 \left(\frac{6}{5} + \frac{9a\omega}{32}\right) + \dots, \quad (58)$$

$$\frac{a_3^{(1)}}{a_0^{(1)}} = -\frac{(a\omega)^3}{32} \left(\frac{65}{3} + \frac{1247}{200}a\omega\right) + \dots. \quad (59)$$

## A.3 Scalar Fields

We finally study the case of scalar fields ( $h = 0$ ). For our analysis, we will need the sum coefficients  $a_p$  for the modes  $l = m = 0$  and  $l = m = 1$ . We start with the case with  $l = m = 0$ : employing again Eq. (24) and (28), we find the following results for the angular eigenvalue

$${}_0A_{00} = -\frac{(a\omega)^2}{3}, \quad (60)$$



and the  $(\alpha_p, \beta_p, \gamma_p)$  coefficients

$$\alpha_p = -2(p+1)^2, \quad \beta_p = p(p+1) - a\omega(4p+2) - \frac{2(a\omega)^2}{3}, \quad \gamma_p = 2a\omega p, \quad (61)$$

that, in turn, lead to the following relations between the first five sum coefficients  $a_p$

$$\frac{a_1^{(00)}}{a_0^{(00)}} = -a\omega \left(1 + \frac{a\omega}{3}\right), \quad \frac{a_2^{(00)}}{a_0^{(00)}} = \frac{(a\omega)^2}{3} \left(2 + a\omega + \frac{(a\omega)^2}{12}\right), \quad (62)$$

$$\frac{a_3^{(00)}}{a_0^{(00)}} = -\frac{(a\omega)^3}{3} \left(1 + \frac{65a\omega}{108}\right) + \dots, \quad \frac{a_4^{(00)}}{a_0^{(00)}} = \frac{(a\omega)^4}{108} \left(\frac{115}{8} + \frac{29a\omega}{3}\right) + \dots \quad (63)$$

For the mode  $l = m = 1$ , a similar analysis leads to the following results for the eigenvalue

$${}_0A_{11} = 2 - \frac{(a\omega)^2}{5}, \quad (64)$$

the  $(\alpha_p, \beta_p, \gamma_p)$  coefficients

$$\alpha_p = -2(p+1)(p+2), \quad \beta_p = p(p+3) - 4a\omega(p+1) - \frac{4(a\omega)^2}{5}, \quad \gamma_p = 2a\omega(p+1), \quad (65)$$

and the first five sum coefficients  $a_p$

$$\frac{a_1^{(11)}}{a_0^{(11)}} = -a\omega \left(1 + \frac{a\omega}{5}\right), \quad \frac{a_2^{(11)}}{a_0^{(11)}} = \frac{(a\omega)^2}{5} \left(3 + a\omega + \frac{(a\omega)^2}{15}\right), \quad (66)$$

$$\frac{a_3^{(11)}}{a_0^{(11)}} = -\frac{(a\omega)^3}{15} \left(4 + \frac{103a\omega}{60}\right) + \dots, \quad \frac{a_4^{(11)}}{a_0^{(11)}} = \frac{(a\omega)^4}{300} \left(\frac{571}{20} + \frac{43a\omega}{3}\right) + \dots \quad (67)$$

## References

- [1] N. Arkani-Hamed, S. Dimopoulos and G. R. Dvali, *Phys. Lett. B* **429**, 263 (1998) [hep-ph/9803315]; *Phys. Rev. D* **59**, 086004 (1999) [hep-ph/9807344];  
I. Antoniadis, N. Arkani-Hamed, S. Dimopoulos and G. R. Dvali, *Phys. Lett. B* **436**, 257 (1998) [hep-ph/9804398].
- [2] T. Banks and W. Fischler, hep-th/9906038.
- [3] S. W. Hawking, *Commun. Math. Phys.* **43**, 199 (1975).
- [4] P. Kanti, *Int. J. Mod. Phys. A* **19**, 4899 (2004) [hep-ph/0402168]; *Lect. Notes Phys.* **769**, 387 (2009) [arXiv:0802.2218 [hep-th]]; *J. Phys. Conf. Ser.* **189** (2009) 012020 [arXiv:0903.2147 [hep-th]]; *Rom. J. Phys.* **57** (2012) 96 [arXiv:1204.2371 [hep-th]].
- [5] M. Cavaglia, *Int. J. Mod. Phys. A* **18**, 1843 (2003) [hep-ph/0210296];  
G. L. Landsberg, *Eur. Phys. J. C* **33**, S927 (2004) [hep-ex/0310034];  
K. Cheung, hep-ph/0409028;  
S. Hossenfelder, hep-ph/0412265;

- A. S. Majumdar and N. Mukherjee, *Int. J. Mod. Phys. D* **14**, 1095 (2005) [astro-ph/0503473];  
 E. Winstanley, arXiv:0708.2656 [hep-th];  
 S. C. Park, *Prog. Part. Nucl. Phys.* **67** (2012) 617 [arXiv:1203.4683 [hep-ph]].
- [6] C. M. Harris, hep-ph/0502005.
- [7] P. Kanti and J. March-Russell, *Phys. Rev. D* **66**, 024023 (2002) [hep-ph/0203223]; *Phys. Rev. D* **67**, 104019 (2003) [hep-ph/0212199].
- [8] V. P. Frolov and D. Stojkovic, *Phys. Rev. D* **66**, 084002 (2002) [hep-th/0206046].
- [9] C. M. Harris and P. Kanti, *JHEP* **0310**, 014 (2003) [hep-ph/0309054].
- [10] A. S. Cornell, W. Naylor and M. Sasaki, *JHEP* **0602**, 012 (2006) [hep-th/0510009];  
 V. Cardoso, M. Cavaglia and L. Gualtieri, *Phys. Rev. Lett.* **96**, 071301 (2006) [hep-th/0512002]; *JHEP* **0602**, 021 (2006) [hep-th/0512116];  
 S. Creek, O. Efthimiou, P. Kanti and K. Tamvakis, *Phys. Lett. B* **635**, 39 (2006) [hep-th/0601126];  
 D. C. Dai, N. Kaloper, G. D. Starkman and D. Stojkovic, *Phys. Rev. D* **75**, 024043 (2007) [hep-th/0611184].
- [11] P. Kanti, J. Grain and A. Barrau, *Phys. Rev. D* **71** (2005) 104002 [hep-th/0501148].
- [12] J. Grain, A. Barrau and P. Kanti, *Phys. Rev. D* **72** (2005) 104016 [hep-th/0509128].
- [13] P. Nicolini and E. Winstanley, *JHEP* **1111** (2011) 075 [arXiv:1108.4419 [hep-ph]].
- [14] C. M. Harris and P. Kanti, *Phys. Lett. B* **633** (2006) 106 [hep-th/0503010];  
 G. Duffy, C. Harris, P. Kanti and E. Winstanley, *JHEP* **0509**, 049 (2005) [hep-th/0507274].
- [15] M. Casals, P. Kanti and E. Winstanley, *JHEP* **0602**, 051 (2006) [hep-th/0511163];
- [16] M. Casals, S. Dolan, P. Kanti and E. Winstanley, *JHEP* **0703**, 019 (2007) [hep-th/0608193].
- [17] D. Ida, K. y. Oda and S. C. Park, *Phys. Rev. D* **67**, 064025 (2003) [Erratum-ibid. *D* **69**, 049901 (2004)] [hep-th/0212108]; *Phys. Rev. D* **71**, 124039 (2005) [hep-th/0503052]; *Phys. Rev. D* **73**, 124022 (2006) [hep-th/0602188].
- [18] S. Creek, O. Efthimiou, P. Kanti and K. Tamvakis, *Phys. Rev. D* **75** (2007) 084043 [hep-th/0701288].
- [19] S. Creek, O. Efthimiou, P. Kanti and K. Tamvakis, *Phys. Rev. D* **76** (2007) 104013 [arXiv:0707.1768 [hep-th]].
- [20] V. P. Frolov and D. Stojkovic, *Phys. Rev. D* **67**, 084004 (2003) [gr-qc/0211055];  
 H. Nomura, S. Yoshida, M. Tanabe and K. i. Maeda, *Prog. Theor. Phys.* **114**, 707 (2005) [hep-th/0502179].  
 T. Kobayashi, M. Nozawa, Y. Takamizu, *Phys. Rev. D* **77**, 044022 (2008) [arXiv:0711.1395 [hep-th]];  
 S. Chen, B. Wang, R. K. Su and W. Y. Hwang, *JHEP* **0803**, 019 (2008) [arXiv:0711.3599 [hep-th]].

- [21] S. Creek, O. Efthimiou, P. Kanti and K. Tamvakis, *Phys. Lett. B* **656**, 102 (2007) [arXiv:0709.0241 [hep-th]];
- [22] M. Casals, S. R. Dolan, P. Kanti and E. Winstanley, *JHEP* **0806**, 071 (2008) [arXiv:0801.4910 [hep-th]].
- [23] H. Kodama, *Prog. Theor. Phys. Suppl.* **172**, 11 (2008) [arXiv:0711.4184 [hep-th]]; *Lect. Notes Phys.* **769**, 427 (2009) [arXiv:0712.2703 [hep-th]];  
J. Doukas, H. T. Cho, A. S. Cornell and W. Naylor, *Phys. Rev. D* **80** (2009) 045021 [arXiv:0906.1515 [hep-th]];  
P. Kanti, H. Kodama, R. A. Konoplya, N. Pappas and A. Zhidenko, *Phys. Rev. D* **80** (2009) 084016 [arXiv:0906.3845 [hep-th]].
- [24] E. Jung and D. K. Park, *Nucl. Phys. B* **731**, 171 (2005) [hep-th/0506204]; *Mod. Phys. Lett. A* **22**, 1635 (2007) [hep-th/0612043].
- [25] M. O. P. Sampaio, *JHEP* **0910** (2009) 008 [arXiv:0907.5107 [hep-th]]; *JHEP* **1002** (2010) 042 [arXiv:0911.0688 [hep-th]].
- [26] P. Kanti and N. Pappas, *Phys. Rev. D* **82** (2010) 024039 [arXiv:1003.5125 [hep-th]].
- [27] J. A. Frost, J. R. Gaunt, M. O. P. Sampaio, M. Casals, S. R. Dolan, M. A. Parker and B. R. Webber, *JHEP* **0910** (2009) 014 [arXiv:0904.0979 [hep-ph]].
- [28] D-C. Dai, G. Starkman, D. Stojkovic, C. Issever, E. Rizvi, and J. Tseng, *Phys. Rev. D* **77**, 076007 (2008) [arXiv:0711.3012 [hep-ph]].
- [29] A. Flachi, M. Sasaki and T. Tanaka, *JHEP* **0905** (2009) 031 [arXiv:0809.1006 [hep-ph]].
- [30] M. Casals, S. R. Dolan, P. Kanti and E. Winstanley, *Phys. Lett. B* **680** (2009) 365 [arXiv:0907.1511 [hep-th]].
- [31] M. O. P. Sampaio, *JHEP* **1203** (2012) 066 [arXiv:1201.2422 [hep-ph]].
- [32] D. C. Dai and D. Stojkovic, *JHEP* **1008** (2010) 016 [arXiv:1008.4586 [gr-qc]].
- [33] R. C. Myers and M. J. Perry, *Annals Phys.* **172**, 304 (1986).
- [34] S. A. Teukolsky, *Phys. Rev. Lett.* **29**, 1114 (1972); *Astrophys. J.* **185**, 635 (1973).
- [35] W. H. Press and S. A. Teukolsky, *Astrophys. J.* **185**, 649 (1973).
- [36] E. D. Fackerell and R. G. Grossman, *J. Math. Phys.* **18**, 1849 (1977).
- [37] A. A. Starobinskii and S. M. Churilov, *Sov. Phys.-JETP* **38**, 1 (1974).
- [38] E. Seidel, *Class. Quant. Grav.* **6**, 1057 (1989).
- [39] E. Berti, V. Cardoso and M. Casals, *Phys. Rev. D* **73** (2006) 024013 [Erratum-ibid. *D* **73** (2006) 109902];
- [40] E. W. Leaver, *Proc. Roy. Soc. London A* **402**, 285 (1985).